Eur. Phys. J. C 16, 683–693 (2000)
Digital Object Identifier (DOI) 10.1007/s100520000442

THE EUROPEAN PHYSICAL JOURNAL C

Angular pattern of minijet transverse energy flow in hadron and nuclear collisions

A.V. Leonidov[1,2], D.M. Ostrovsky[1]

[1] P.N. Lebedev Physics Institute, 117924 Leninsky pr. 53, Moscow, Russia
[2] Service de Physique Theorique, C.E. Saclay, 91191 Gif-sur-Yvette, France

Received: 19 January 1999 / Revised version: 18 February 2000 /
Published online: 26 July 2000 – © Springer-Verlag 2000

Abstract. The azimuthal asymmetry of a minijet system produced at the early stage of nucleon–nucleon and nuclear collisions in a central rapidity window is studied. We show that in pp collisions the minijet transverse energy production in a central rapidity window is essentially unbalanced in the azimuth due to asymmetric contributions in which only one minijet hits the acceptance window. We further study the angular pattern of the transverse energy flow generated by the semihard degrees of freedom at the early stage of high energy nuclear collisions and its dependence on the number of semihard collisions in the models both including and neglecting soft contributions to the inelastic cross section at RHIC and LHC energies as well as on the choice of the infrared cutoff.

1 Introduction

Minijet physics is one of the most promising applications of perturbative QCD to the analysis of processes with multiparticle production. It addresses the crucial question of how many (semi)hard degrees of freedom can be available in a given event. The approach is based on the idea that some portion of the transverse energy is produced in the semihard form, i.e., is perturbatively calculable because of the relatively large transverse momenta involved in the scattering, but, due to parametrically strong hadronization effects, cannot be observed in the form of customary well collimated hard jets distinctly separable from the soft background. This mechanism operates at the early stage of the collision and, when relevant, determines the characteristics of the primordial transverse energy flow.

The creation of many (semi)hard degrees of freedom corresponds to a new physical situation characterized by nontrivial, possibly kinetic, or even hydrodynamic, phenomena occurring at the parton level at the early stages of a high energy collision. Of special relevance are here the ultrarelativistic heavy ion collisions, where one would expect that creating a dense system of (semi)hard degrees of freedom in the volume much larger than, e.g., the proton one, is possible, thus making the application of concepts borrowed from macroscopic physics natural. A recent critical discussion of this field can be found in [1].

Minijet physics is an actively developing field. Reviews on the subject containing a large number of references are, e.g., [2–4]. Several approaches have been considered with the aim of providing a quantitative description of a primordial parton system produced at the earliest stage of, e.g., high energy heavy ion collisions. The conceptually simplest one is based on the standard formalism of collinearly factorized QCD at small parton densities; see [5–9]. Here one operates with a single hard parton–parton scattering in a given hadron–hadron collision, so that standard QCD structure functions can be used in computing the probability of generating a pair of partons with certain kinematical characteristics.

This approach has a natural generalization, in which multiple binary parton–parton collisions in the given hadron–hadron one are considered, provided some ad hoc distribution in the number of these collisions is chosen; see e.g. [10]. This also allows one to construct a geometrically motivated scheme of unitarizing the semihard contribution to the inelastic cross section of hadron scattering, as described, e.g., in [3].

Starting from [11], nonlinear QCD effects in relation with describing the early stages of heavy ion collisions drew progressively more and more attention. New results were obtained within the approach to minijet production based on the quasiclassical treatment of nuclear gluon distributions within a framework of McLerran–Venugopalan model [12]; see also [13–17]. First nonperturbative results on gluon production are now available [18]; see also [19, 20]. Recently a nonperturbative model for gluon production in heavy ion collisions based on the physical concepts of the McLerran–Venugopalan model and a corresponding kinetic equation describing the evolution of a primordial gluon system were discussed in [21]. For a pedagogical introduction to this rapidly developing field see the lectures in [22,23].

A notable feature of the physical phenomena related to the collective behavior of multiparton systems is their genuine event-by-event nature, so that many usual tools used

in high energy physics, such as inclusive distributions, are becoming less helpful. Thus the analysis of event-by-event variations of the quantities sensitive to the collective dynamics is very important; see [24–27] and references therein.

The description of the primordial parton configuration should provide information on the event-by-event pattern of the parton system, in particular on the number of perturbative parton producing interactions, which, to a large extent, determines the initial parton density and other kinematical characteristics. In particular, the discrete nature of parton production in phase space, as described by finite order QCD calculations, can give rise to primordial event-by-event angular asymmetries of the parton flow. The fate of the primordial angular asymmetries depends on the relevant dynamics (Is the evolution of the produced system long enough to wash them out? Can they be frozen and can they be directly relevant to the observed hadronic flow? Etc.). In any case the first problem to look at is to study the primordial parton system before the reinteraction of partons sets in.

The aim of this paper is to study the characteristics of the initial minijet-induced transverse energy flow in nucleon–nucleon and nucleus–nucleus collisions within the framework of a minijet production scenario based on collinearly factorized QCD [5, 6]. In particular, we shall analyze the fluctuational azimuthal imbalance in the minijet transverse energy flow due to the discrete nature of transverse energy production through basic QCD hard scattering. We can expect that this effect will be essentially sensitive to the number of semihard scatterings. In what follows we shall see that this is indeed the case.

Below we study the event-by-event inhomogeneities in the azimuthal distribution of minijets following from the basic asymmetry of minijet transverse energy production into a finite rapidity window in *pp* collisions. The nuclear collisions are described by a geometric model [6] in which they are considered as a superposition of basic nucleon–nucleon ones. The azimuthal asymmetry of the minijet system will be specified in terms of (transverse) momenta only, as calculated in the conventional S-matrix field theory formalism without referring to the coordinates of the partons and making no assumptions on the structure of the contributions of higher order in the QCD coupling constant in describing the transverse energy production in the elementary nucleon–nucleon collision. This analysis can be extended to the next-to-leading order (e.g. along the lines of [28]) due to the infrared stability of the considered distributions which are of energy–energy correlation type.

The analysis of the event-by-event pattern of the initial minijet generated transverse energy flow was first presented in [29], where a HIJING [30] generated list of partons with specified coordinates and momenta was used to compute a coarse-grained energy density and velocity field at RHIC energy $s^{1/2} = 200\,\mathrm{GeV}$. The resulting distributions turned out to be highly irregular and similar to the ones occurring in turbulent flows. Note that besides the parton–parton scattering described by collinearly factorized QCD considered in the present paper, HIJING makes explicit assumptions on the structure of higher order contributions (unitarization), the contribution from initial and final state radiation and the structure of the parton system in coordinate space (thus going beyond the standard S-matrix formalism). The existence of asymmetry due to imbalanced particle production from minijets into a finite acceptance was mentioned in [3].

The outline of this paper is as follows.

In the second section we analyze the basic mechanism for producing azimuthally symmetric and asymmetric configurations in the restricted phase space domain, which in the considered case will be a unit central rapidity window, in *pp* collisions. We calculate in the leading twist (lowest order in parton density) and leading order collinear factorization scheme the relative weights for symmetric (two-jet) and asymmetric (one-jet) contributions to the transverse energy production cross section for RHIC ($s^{1/2} = 200\,\mathrm{GeV}$) and LHC ($s^{1/2} = 5500\,\mathrm{GeV}$) for the underlying nucleon–nucleon collisions.

In the third section the computed contributions to azimuthally symmetric and asymmetric components of the *pp* minijet transverse energy production into a unit central rapidity window are used in calculating the asymmetry of the transverse energy production in heavy ion collisions, where the nuclear collision is described as a superposition of the nucleon–nucleon ones in the geometrical approach of [6]. We study the azimuthal asymmetry for RHIC and LHC energies for central collisions for two dynamical scenarios. In the first scenario the transverse energy production is assumed to occur through two physically different mechanisms, the soft one and the (semi)hard one. As our aim is to study the transverse energy flow at an early collision stage related to the semihard degrees of freedom, the contribution of soft interactions will be accounted for only in determining the relative yield of the semihard contribution. In the second scenario, which can become realistic at LHC energies, all primordial transverse energy production is assumed to occur through the semihard mechanism.

In the last section we discuss the results and formulate the conclusions.

2 Azimuthal pattern of minijet production in *pp* collisions

The mechanism responsible for transverse energy production in the leading order in QCD perturbation theory is elastic two-to-two parton–parton scattering. Its cross section is given by the standard collinearly factorized expression

$$\frac{\mathrm{d}\sigma}{\mathrm{d}p_\perp^2\,\mathrm{d}y_1\mathrm{d}y_2} = x_1 f(x_1, p_\perp^2)\frac{\mathrm{d}\hat{\sigma}}{\mathrm{d}p_\perp^2} x_2 f(x_2, p_\perp^2), \qquad (1)$$

where $xf(x, p_\perp^2)$ is a parton structure function, $x_{1,2} = p_\perp(\mathrm{e}^{\pm y_1} + \mathrm{e}^{\pm y_2})/S^{1/2}$ are the fractional longitudinal momenta of the produced partons and $\mathrm{d}\hat{\sigma}/\mathrm{d}p_\perp^2$ is the differential cross section of elastic parton–parton scattering. In the following we will specifically be interested in the

transverse energy production into some given (central) rapidity interval $y_{\min} < y_1, y_2 < y_{\max}$. Operationally the transverse energy $E_\perp$ deposited in this window by the two scattered partons is defined as[1]

$$E_\perp = p_1\theta(y_{\min} \le y_1 \le y_{\max}) + p_2\theta(y_{\min} \le y_2 \le y_{\max}). \quad (2)$$

Let us stress that while the expression of the transverse energy in (2) is specifically taken to be of the lowest order in α_s, the quantity $E_\perp$ refers to the total transverse energy produced in a particular rapidity interval in a semihard collision. In the following we shall confine ourselves to considering the central rapidity interval $y_{\min} = -0.5 < y < y_{\max} = 0.5$ and stay at the LO (Born elastic scattering) level, so that in each collision the transverse momenta of the two produced partons are equal, $p_{\perp 1} = p_{\perp 2} = p$. This *does not* mean that these transverse momenta will be balanced in the rapidity window under consideration, so the event space for transverse energy deposition can be summarized by

$$E_\perp = \begin{cases} 0 \text{ if no particle gets into the gap,} \\ p \text{ if one particle gets into the gap,} \\ 2p \text{ if two particles get into the gap.} \end{cases} \quad (3)$$

When considering the transverse energy production into a given rapidity window in pp collisions only the second and third possibilities are relevant. To quantify the computation of the contribution corresponding to cases 2 and 3 in (3) it is convenient to introduce the integral operators

$$S_1 = \int \mathrm{d}y_1 \mathrm{d}y_2 (\theta(y_1) + \theta(y_2) - 2\theta(y_1)\theta(y_2)) * (\ldots) \quad (4)$$

$$S_2 = \int \mathrm{d}y_1 \mathrm{d}y_2 (\theta(y_1)\theta(y_2)) * (\ldots), \quad (5)$$

where $\theta(y_{1,2}) = \theta(y_{\min} < y_{1,2} < y_{\max})$ Applying these operators to the differential cross section (1) we get a decomposition of the transverse energy production cross section in a given rapidity window into the separate one-jet and two-jet contributions (second and third entries in the event list (3));

$$\frac{\mathrm{d}\sigma}{\mathrm{d}E_\perp} = \frac{\mathrm{d}\sigma_1}{\mathrm{d}E_\perp} + \frac{\mathrm{d}\sigma_2}{\mathrm{d}E_\perp}, \quad (6)$$

where

$$\frac{\mathrm{d}\sigma_1}{\mathrm{d}E_\perp} = S_1 * \left(\frac{\mathrm{d}\sigma}{\mathrm{d}p}\right)\Big|_{p=E_\perp}, \quad (7)$$

and

$$\frac{\mathrm{d}\sigma_2}{\mathrm{d}E_\perp} = 2S_2 * \left(\frac{\mathrm{d}\sigma}{\mathrm{d}p}\right)\Big|_{p=E_\perp/2}. \quad (8)$$

On the event-by-event basis these contributions correspond to completely distinct possibilities of having the azimuthally balanced symmetric or unbalanced asymmetric transverse energy flow in the rapidity window under consideration.

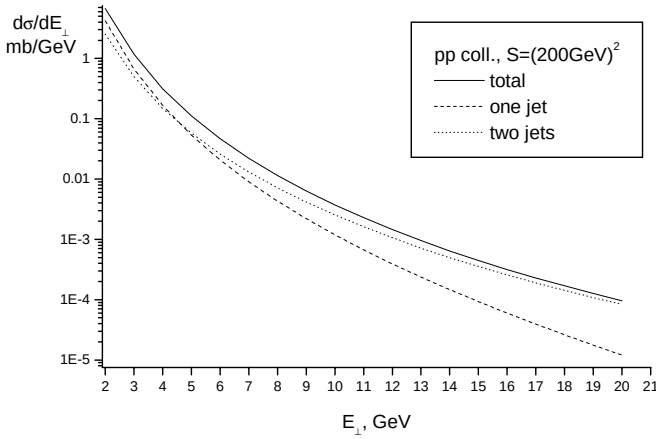

Fig. 1. One and two jets contributions to transverse energy production in pp collisions in a unit central rapidity window at RHIC energy $s^{1/2} = 200\,\mathrm{GeV}$

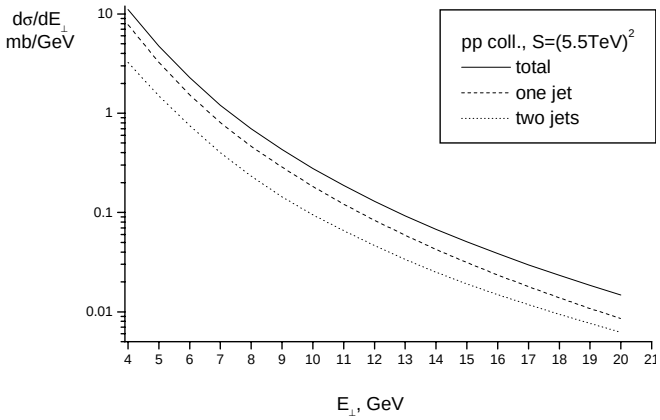

Fig. 2. One and two jets contributions to transverse energy production in pp collisions in a unit central rapidity window at LHC energy $s^{1/2} = 5500\,\mathrm{GeV}$

We emphasize that the cross section in (2) is an exclusive one and is infrared stable, $E_\perp$ being the total transverse energy deposited in a given rapidity interval. In Figs. 1 and 2 we plot the transverse energy production cross sections (7) and (8) produced both by gluon and quark (with $n_f = 5$) minijets for RHIC and LHC energies $s^{1/2} = 200\,\mathrm{GeV}$ and $s^{1/2} = 5500\,\mathrm{GeV}$, where for LHC we have chosen the energy to be available for protons in lead beams, and the MRSG structure functions [31] were used.

In Fig. 3 we also present the differential cross sections of the transverse energy production into full rapidity intervals available at RHIC and LHC energies which will be used in the next section to normalize the differential cross sections of the transverse energy production in pp collisions.

The information contained in Figs. 1 and 2 is summarized in Table 1, where we show the parameters for the fits for the one-jet and two-jet spectra, (7) and (8) having the functional form $c(E_\perp/1\,\mathrm{GeV})^{-\alpha}$.

[1] In (2) and below $p_i = |\mathbf{p}_{\perp i}|$

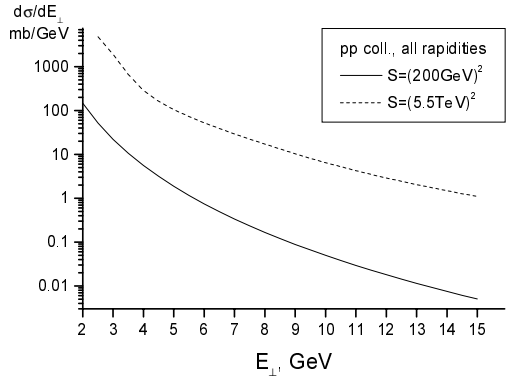

Fig. 3. Transverse energy production in pp collisions in the whole rapidity interval at RHIC ($s^{1/2} = 200\,\mathrm{GeV}$) and LHC ($s^{1/2} = 5.5\,\mathrm{TeV}$) energies

Table 1.

$S^{1/2}$, GeV	α_1	α_2	c, mb/GeV	
	1 jet	2 jets	1 jet	2 jets
200	5.09	4.53	173	77
5500	4.25	3.93	3099	819

We see that at RHIC energies the one-jet asymmetric contribution dominates at small transverse energies, and at $E_\perp \sim 4.5\,\mathrm{GeV}$ the two-jet symmetric contribution takes over. At LHC energies the asymmetric contribution is clearly dominant in the whole minijet transverse energy range.

3 Azimuthal asymmetry of minijet transverse energy flow in nuclear collisions

In this section we turn to the analysis of the angular asymmetry of minijet produced transverse energy flow in nuclear collisions induced by the fundamental asymmetry in the pp collisions described in the previous section. The translation of the features characterizing the particle production in pp collisions to those characterizing the nuclear ones is possible, e.g., in a geometrical model, where the nucleus–nucleus collision is considered as a superposition of the proton–proton ones, see e.g. [5,6]. At each impact parameter b, where b is a distance in the transverse plane between the centers of the colliding nuclei, the nucleus–nucleus collision is described as a Poissonian superposition of nucleon–nucleon collisions such that a probability of n pp collisions is given by

$$w_n(b) = \frac{1}{n!}\bar{N}_{AB}^n(b)\mathrm{e}^{-\bar{N}_{AB}(b)}, \tag{9}$$

where $\bar{N}_{AB}(b)$ is the average number of pp collisions in the nucleus–nucleus one, which is thus described as a specific superposition of multiple independent pp collisions occurring with the weight given by (9). The elementary pp collisions occur between some nucleon belonging to the nucleus A located at the transverse distance b_1 from its center with the probability given by the probability density $\rho_A(b_1)$ with the normalization

$$\int \mathrm{d}^2 b_1 \rho_A(b_1) = 1, \tag{10}$$

and the nucleon from nucleus B located at the transverse distance b_2 from its center with the probability given by the probability density $\rho_B(b_2)$ with the collision probability $P\left(\bar{b} - \bar{b}_1 + \bar{b}_2\right)$. Thus the average number of pp collisions characterizing the basic Poissonian process (9) is given by

$$\bar{N}_{AB}(b) = AB \int \mathrm{d}^2 b_1 \mathrm{d}^2 b_2 P\left(\bar{b} - \bar{b}_1 + \bar{b}_2\right) \rho_A(b_1)\rho_B(b_2), \tag{11}$$

where $P(b)$ is the probability of an inelastic collision of two nucleons initially separated by the transverse distance $\bar{b}-\bar{b}_1+\bar{b}_2$. In practical calculations we use the Wood–Saxon nuclear probability density [32].

The physical meaning of the collision probability $P(b)$ depends on the underlying physical mechanism responsible for inelastic transverse energy production in the binary nucleon–nucleon collisions. Our discussion is confined to minijets as providing such a source, so in our case $P(b)$ is a probability of minijet producing inelastic nucleon–nucleon collision occurring at fixed impact parameter b. Let us stress that the differential probability of the minijet-induced transverse energy production depends on the rapidity window under consideration. The usual assumption about the impact parameter dependence of the probability of nucleon–nucleon collisions $P(b)$ is that the collisions are local in the impact parameter plane, i.e.

$$P(b) = \sigma_{pp}^{\mathrm{minijet}}(|\Delta y| \le y_0)\delta^{(2)}(b). \tag{12}$$

Let us now discuss in some detail the normalization of the Poisson process (9) provided by the overall minijet production cross section into the rapidity window $|\Delta y| \le y_0$, $\sigma_{pp}^{\mathrm{minijet}}(|\Delta y| \le y_0)$. The overall minijet contribution to the transverse energy production cross section is given by the integral over $E_\perp$ of the differential cross section (6). Because of the singular behavior of the perturbative transverse energy production cross section at small $E_\perp$, the very definition of the overall contribution of the minijet mechanism of the transverse energy production requires introducing a cutoff at small transverse energies,

$$\sigma_{pp}^{\mathrm{minijet}}(|\Delta y| \le y_0|E_0) = \int_{E_0} \mathrm{d}E_\perp \frac{\mathrm{d}\sigma}{\mathrm{d}E_\perp}(\Delta y). \tag{13}$$

Let us note that for any rapidity interval

$$\int_{E_0} \mathrm{d}E_\perp \frac{\mathrm{d}\sigma}{\mathrm{d}E_\perp}(\Delta y) \le \sigma^{\mathrm{inel}}(\Delta y), \tag{14}$$

where $\sigma^{\mathrm{inel}}(\Delta y)$ is an (experimental) inelastic cross section in a given rapidity window Δy. This shows that the cutoff E_0 is physically a function of the considered rapidity interval.

Another important issue related to the choice of this cutoff is the possible contribution to the overall inelastic cross section of other mechanisms of transverse energy production, e.g. of the soft particle production due to the decay of hadronic strings. The restriction (14) clearly refers only to the part of the inelastic cross section corresponding to hard inelasticity, i.e. the transverse energy production through semihard processes. The other part of the inelastic cross section corresponds to soft mechanisms of transverse energy production which do not involve large momentum transfers. It is important to note that the characteristic time scale of the semihard transverse energy production is smaller than that for the soft nonperturbative mechanism. At the early stages of the collision a hard parton skeleton is formed, which is then dressed by soft particle production due to strings stretching in between the partons originating from primordial processes characterized by large momentum transfer. This shows, in particular, that the soft processes do not have, generally speaking, an independent share of the overall inelasticity, so the naive additivity

$$\frac{\mathrm{d}\sigma}{\mathrm{d}E_\perp} = \frac{\mathrm{d}\sigma^{\mathrm{minijet}}}{\mathrm{d}E_\perp} + \frac{\mathrm{d}\sigma^{\mathrm{soft}}}{\mathrm{d}E_\perp} \tag{15}$$

is, in general, not valid. It could happen, e.g., that with growing collision energy the yield of events with hard initial inelasticity would be dominant or even cover the whole event space (here we refer to the nondiffractive contribution). In such an extreme scenario the *only* function of the soft mechanism is stretching the strings between the *hard* initial partons. Here it is important to recall that the cross section of transverse energy production (6), as computed in perturbative QCD, is a so-called infrared safe quantity and is thus entirely determined by its early quark–gluon stage and does not depend on the late stages of the process, including string formation between the separating partons.

Let us stress once again that in the present study we confine our consideration to analyzing the angular pattern of the primordial transverse energy flow generated at the early stages of the collisions by the semihard degrees of freedom (minijets). The analysis of the effects related to the subsequent redistribution of the primordial transverse energy by soft interactions at larger times will be discussed in future publications [33].

The yield of the perturbative contribution as a function of the CMS energy is a crucial characteristic of the inelastic cross section. Unfortunately very little can currently be said about its magnitude, resulting in the uncertainty in fixing the cutoff for the perturbative contribution.

In view of this we shall fix the cutoff value E_0 at given collision energy as follows. To explore the possible "window of opportunities" for the hard minijet contribution as determined by the yield of independent soft particle production we will discuss two model scenarios. Namely, when considering the inelastic particle production at all rapidities we shall either assume the constant soft contribution $\sigma^{\mathrm{soft}}(pp) = 32\,\mathrm{mb}$, the inelastic cross section of pp scattering at intermediate energies, universally present at all CMS energies (mixed scenario), or we shall assume that in all collisions the transverse energy is produced via the early perturbative minijet stage, i.e. we put $\sigma^{\mathrm{soft}}(pp) = 0$ (hard scenario). The cutoff E_0 is thus determined from[2]

$$\int_{E_0} \mathrm{d}E_\perp \frac{\mathrm{d}\sigma_{pp}^{\mathrm{minijet}}}{\mathrm{d}E_\perp} = \sigma^{\mathrm{hard}} = \begin{cases} \sigma_{\mathrm{exp}}^{\mathrm{inel}}, & \text{no soft contribution} \\ \sigma_{\mathrm{exp}}^{\mathrm{inel}} - 32\,\mathrm{mb}, & \text{soft contribution } 32\,\mathrm{mb}, \end{cases} \tag{16}$$

where the transverse spectrum in (16) refers to the full kinematic interval (see Fig. 3). Let us stress that the differential cross section for the transverse energy production that we use in (16) is the result of the lowest order calculation from the previous section, and the higher order effects that can phenomenologically be included within the geometrical unitarization scheme, see e.g. [3], are not included. Numerical values of the cutoff found by integrating the spectra shown in Fig. 3 are given in Table 2.

In the fifth column we show the overall probability of the asymmetric one-jet contribution $p_1(E_0)$ calculated using the differential transverse energy production spectra (6), (7) and (8):

$$p_1(E_0) = \left(\int_{E_0}^{\infty} \mathrm{d}E_\perp \frac{\mathrm{d}\sigma_1}{\mathrm{d}E_\perp}\right) \Big/ \left(\int_{E_0}^{\infty} \mathrm{d}E_\perp \frac{\mathrm{d}\sigma}{\mathrm{d}E_\perp}\right). \tag{17}$$

As already mentioned, although the differential spectra describe the transverse energy production into some given rapidity window, in what follows the value of the cutoff E_0 will be determined from (14) considered for the full rapidity window kinematically available for inelastic energy production at a given collision energy. For a more accurate determination of the cutoff E_0 one would need experimental data on the inelastic cross sections in, e.g., the central rapidity window. Different quantities have a different sensitivity with respect to the choice of the cutoff and, in particular, the dependence of $p_1(E_0)$ in (17) on E_0 is quite weak. In the last column in Table 2 we show the cross section of producing at least one minijet in lead–lead collisions $\sigma_{\mathrm{PbPb}}^{\mathrm{minijet}}$:

$$\sigma_{\mathrm{PbPb}}^{\mathrm{minijet}} = \int \mathrm{d}^2b(1 - w_0(b)) = \int \mathrm{d}^2b(1 - \mathrm{e}^{-\bar{N}_{AB}(b)}), \tag{18}$$

where $w_0(b)$ is a probability of having no minijet producing nucleon–nucleon collisions, cf. (9).

The transverse energy production in nucleus–nucleus collisions is then described by the convolution of the distribution over the number of pp collisions obtained from (9) at a given impact parameter with the distributions characterizing the transverse energy production in pp collisions (7) and (8).

[2] The inelastic cross section is computed using the parameterization $\sigma_{\mathrm{inel}}(s) = \sigma_0 \cdot (s/s_0)^{0.0845} \cdot (0.96 - 0.03 \cdot \log(s/s_0))$, where $s_0 = 1\,\mathrm{GeV}$, $\sigma_0 = 21.4\,\mathrm{mb}$, which gives a good description of the existing experimental data [34]; see also the compilation in [3]

Table 2.

$S^{1/2}$, GeV	$\sigma^{\rm soft}$, mb	$\sigma^{\rm hard}$, mb	E_0, GeV	p_1	$\sigma_{pp}^{\rm minijet}$, mb	$\sigma_{\rm PbPb}^{\rm minijet}$, mb
200	0	41.8	2.4	0.54	2.4	5336
	32	9.8	3.5	0.48	0.54	4102
5500	0	66.3	6.9	0.65	2.8	5443
	32	34.3	8.4	0.64	1.5	4970

In practice this convolution was realized by a Monte Carlo procedure, where

(i) a large number (10^7) nucleus–nucleus collisions were generated with the number of pp collisions N distributed according to (9);
(ii) the weight of the one-jet asymmetric (two-jet symmetric) pp collisions is equal to the probability p_1 (respectively $1-p_1$) with p_1 taken from Table 2. More explicitly, this corresponds to a binomial distribution in the number of asymmetric collisions N_a:

$$w(N_a) = C_N^{N_a} p_1^{N_a} (1-p_1)^{N-N_a}; \tag{19}$$

(iii) the weight for $E_\perp$ itself was in turn determined by (7) and (8) for asymmetric and symmetric contributions, respectively;
(iv) the azimuthal orientation of the jet(s) was determined at random corresponding to a flat distribution in the azimuthal angle. For two-jet events the jets are going into opposite directions, so that their azimuths differ by π.

Let us now turn to the quantitative analysis of the event-by-event asymmetry of the minijet-generated transverse energy flow. Our analysis will be made using the (normalized) difference between the transverse energy flow into the oppositely azimuthally oriented sectors with a specified angular opening $\delta\varphi$ each and a rapidity window $|y| < 0.5$. Let us note that this quantity has the important advantage of allowing for the future next-to-leading order analysis. For convenience one can think of the directions of these cones as being "up" and "down" corresponding to some specific choice of the orientation of the system of coordinates in the transverse plane. All our results are, of course, insensitive to the particular choice. Let us denote the transverse energy going into the "upper" and "lower" cones in a given event by $E_\uparrow(\delta\varphi)$ and $E_\downarrow(\delta\varphi)$, respectively. The magnitude of the asymmetry in the transverse energy production can then be quantified by introducing a variable

$$\delta E = E_\uparrow(\delta\varphi) - E_\downarrow(\delta\varphi). \tag{20}$$

Using the distribution over the number of asymmetric collisions (19) and taking into account that the event space of asymmetric collisions is further subdivided into two sets corresponding to nonzero energy going into the upper and lower cone $E_\uparrow$ and $E_\downarrow$, we can calculate the quadratic mean of $\delta E(\delta\phi)$ for the considered azimuthal openings $\delta\phi = \pi/2^n$ $(n = 0, 1, 2)$[3]:

$$\sqrt{\langle \delta E^2 \rangle} = \frac{1}{2^{n/2}} E_0 \sqrt{p_1 \bar{N} \frac{\alpha_1 - 1}{\alpha_1 - 3}}, \tag{21}$$

where α_1 is given in Table 1. The quadratic mean $\delta E(\delta\phi)$ in (21) characterizes the magnitude of the disbalance in the minijet-generated transverse energy flow. Note that δE is essentially sensitive to the overall magnitude of the semihard (minijet generated) transverse energy flow. In (21) this is clearly seen from $\langle \delta E^2 \rangle \propto E_0^2 \bar{N}$. Numerical values for $(\langle \delta E^2 \rangle)^{1/2}$ are presented in Table 4. From now on we confine our discussion to central PbPb collisions.

In Figs. 4–7 we show the probability distribution for δE in central PbPb collisions for the two values of CMS energy of 200 GeV and 5.5 TeV, and two choices for E_0 corresponding to mixed and hard scenarios. The angular apertures were chosen to be π, $\pi/2$ and $\pi/4$. From these figures we see that for all types of collisions (except for Fig. 6) there appear peaks in the probability distribution at the values $\delta E = nE_0$. This is a reflection of the sharp cutoff adopted in the model and the rapid decrease of the minijet cross section with increasing $E_\perp$. In the majority of the cases this effect is seen only for small values of the angular opening. The crucial parameter related to the peaks' appearance is in fact $\bar{N}$. The smaller is $\bar{N}$, the more evident are the peaks. One could expect that hadronization and soft processes accompanying minijet production smoothed away these peaks. Curves that are initially smooth are subject to a Gaussian law with dispersion $\langle \delta E^2 \rangle$. Therefore, we can imagine the appearance of curves with peaks after smoothing with Gaussians with dispersions given by (21). For Fig. 5 the result of such smoothing is shown in the inserted plot.

Another useful quantity is a normalized asymmetry which is, on the contrary, insensitive to the absolute magnitude of the transverse energy flow:

$$r(\delta\varphi) = \frac{E_\uparrow(\delta\varphi) - E_\downarrow(\delta\varphi)}{E_\uparrow(\delta\varphi) + E_\downarrow(\delta\varphi)}, \tag{22}$$

where $r \in [-1, 1]$. In particular, the normalized asymmetry r simplifies on comparing the asymmetries at different CMS energies. The values of $r(\delta\varphi)$ in different collisions are characterized by the normalized probability distribution

$$p(r)|_{\delta\varphi} = \frac{1}{\sigma} \frac{{\rm d}\sigma}{{\rm d}r}\bigg|_{\delta\varphi}. \tag{23}$$

To evaluate $p(r)$ we use a Monte Carlo simulation of the process of nuclear scattering as described above for the generated ensemble of 10^7 PbPb collisions at RHIC and at

[3] It is easy to see that the distribution of δE is a so-called multi-Poisson one

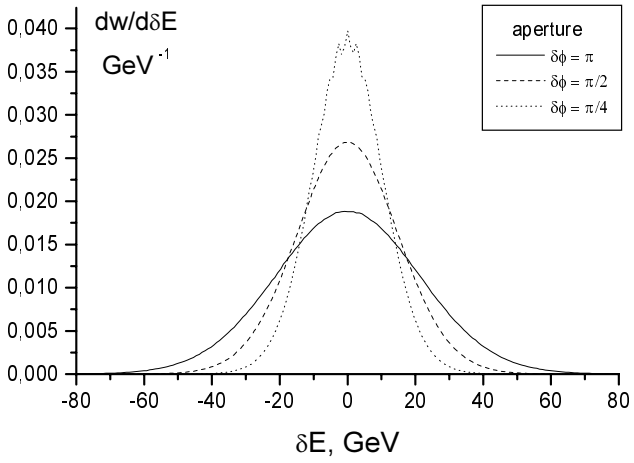

Fig. 4. Probability distribution for the azimuthal asymmetry $\delta E_\perp$ in a unit central rapidity window at RHIC energy $s^{1/2} = 200\,\mathrm{GeV}$ for central PbPb collisions, $\sigma^{\mathrm{soft}} = 0$

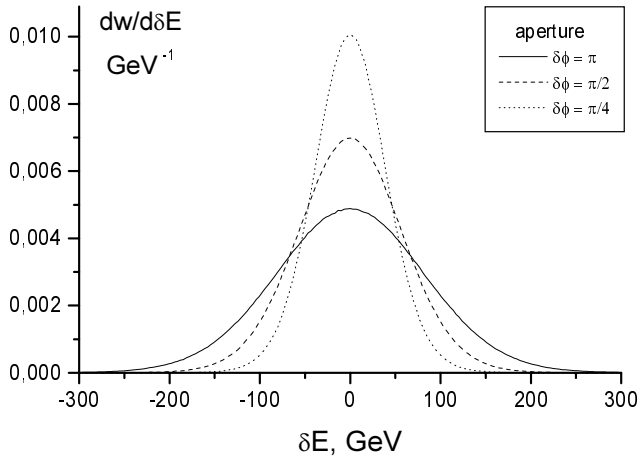

Fig. 6. Probability distribution for the azimuthal asymmetry $\delta E_\perp$ in a unit central rapidity window at LHC energy $s^{1/2} = 5.5\,\mathrm{TeV}$ for central PbPb collisions, $\sigma^{\mathrm{soft}} = 0$

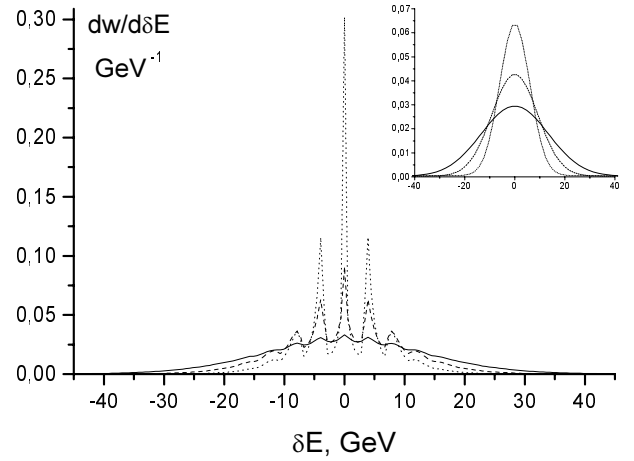

Fig. 5. Probability distribution for the azimuthal asymmetry $\delta E_\perp$ in a unit central rapidity window at RHIC energy $s^{1/2} = 200\,\mathrm{GeV}$ for central PbPb collisions, $\sigma^{\mathrm{soft}} = 32\,\mathrm{mb}$

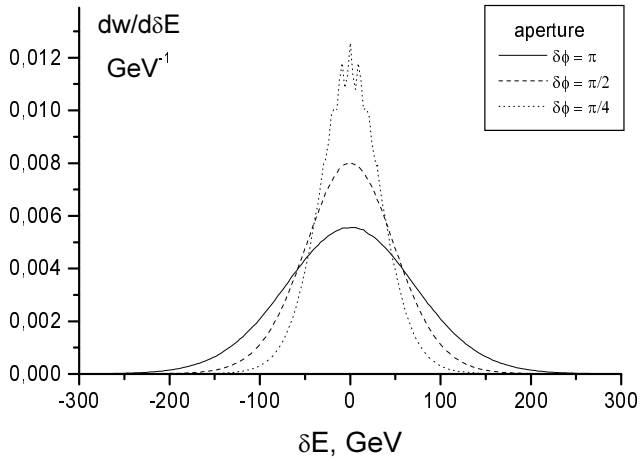

Fig. 7. Probability distribution for the azimuthal asymmetry $\delta E_\perp$ in a unit central rapidity window at LHC energy $s^{1/2} = 5.5\,\mathrm{TeV}$ for central PbPb collisions, $\sigma^{\mathrm{soft}} = 32\,\mathrm{mb}$

LHC energies. We have calculated the asymmetry distributions $p(r)$ for the central (zero impact parameter $b = 0$) collisions and cone apertures $\pi, \pi/2$ and $\pi/4$. The resulting probability distributions are illustrated in Figs. 8–11 for mixed ($\sigma^{\mathrm{soft}} = 32\,\mathrm{mb}$) and hard ($\sigma^{\mathrm{soft}} = 0$) scenarios at RHIC and LHC energies: Let us note that, in particular in the cases where the number of contributing collisions is not large (RHIC), one encounters "singular" configurations, for which $r = -1, 1$ and $r = 0$, corresponding to absolutely asymmetric and absolutely symmetric events in PbPb collisions. These are the events in which only one one-jet event contributes to the given aperture during the collision ($r = -1, 1$) or one two-jet event contributes to $r = 0$. Their probabilistic weight can be described by δ, the functional contribution to $p(r)$ at the "singular" points. Their yield in the minijet event ensemble is given in Table 3 for the mixed ($\sigma^{\mathrm{soft}} = 32\,\mathrm{mb}$) scenario at RHIC energy (other values are negligible).

Table 3.

$\delta\varphi$	$r = -1$	$r = 0$	$r = 1$
$\pi/2$	$1.3 \cdot 10^{-3}$	$1.6 \cdot 10^{-2}$	$1.3 \cdot 10^{-3}$
$\pi/4$	$2.5 \cdot 10^{-2}$	$1.2 \cdot 10^{-1}$	$2.5 \cdot 10^{-2}$

In Fig. 9 these contributions would correspond to infinitely narrow peaks and thus are not shown.

The angular pattern of the transverse energy production as characterized by the considered energy–energy azimuthal correlation probability distribution is conveniently described by the lowest moments of $p(r)$. In Table 4 we present, together with the numerical values of the quadratic mean $(\langle \delta E^2 \rangle)^{1/2}$, cf. (20) and (21), the values of the standard deviation a defined as

$$a^2 = \int \mathrm{d}r (r - \bar{r})^2 p(r), \tag{24}$$

where in our case $\langle r \rangle = 0$:

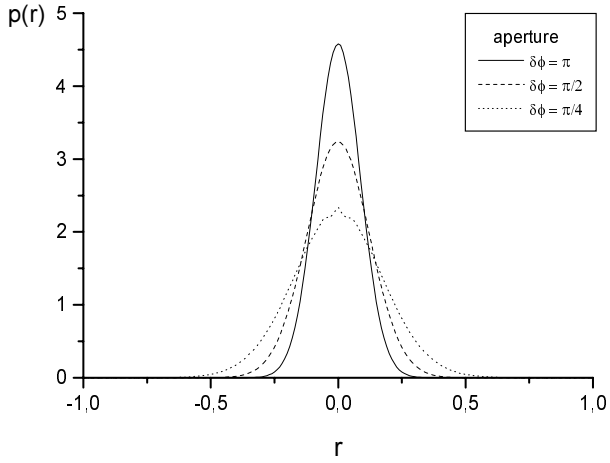

Fig. 8. Probability distribution of the normalized azimuthal asymmetry $p(r)$ in a unit central rapidity window at RHIC energy $s^{1/2} = 200\,\mathrm{GeV}$ for central PbPb collisions, $\sigma^{\mathrm{soft}} = 0$

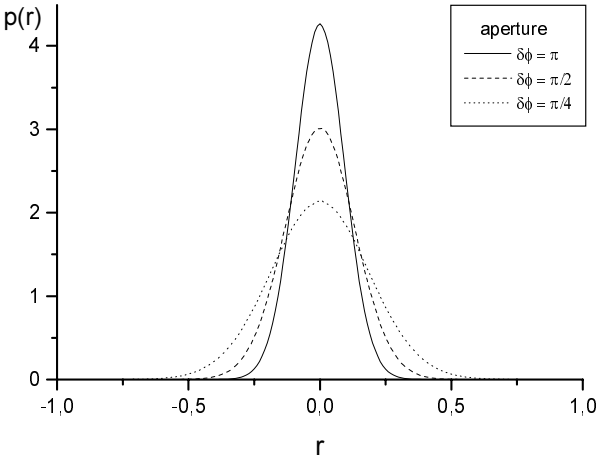

Fig. 10. Probability distribution of the normalized azimuthal asymmetry $p(r)$ in a unit central rapidity window at LHC energy $s^{1/2} = 5.5\,\mathrm{TeV}$ for central PbPb collisions, $\sigma^{\mathrm{soft}} = 0$

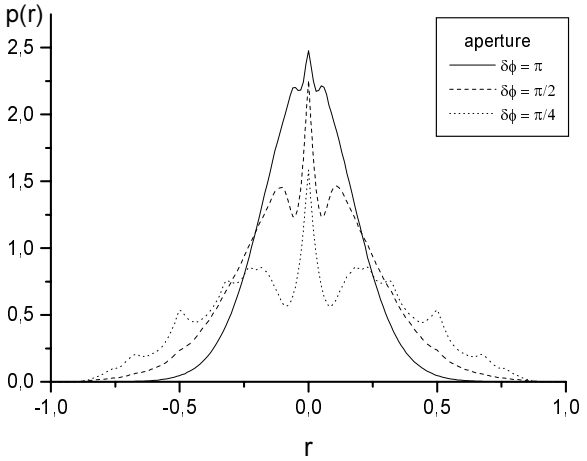

Fig. 9. Probability distribution of the normalized azimuthal asymmetry $p(r)$ in a unit central rapidity window at RHIC energy $s^{1/2} = 200\,\mathrm{GeV}$ for central PbPb collisions, $\sigma^{\mathrm{soft}} = 32\,\mathrm{mb}$

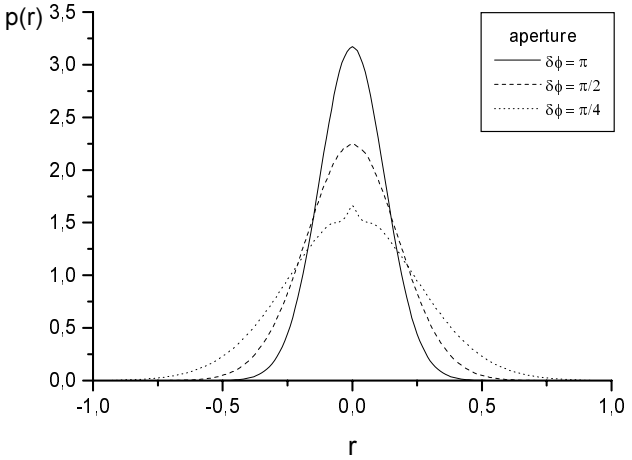

Fig. 11. Probability distribution of the normalized azimuthal asymmetry $p(r)$ in a unit central rapidity window at LHC energy $s^{1/2} = 5.5\,\mathrm{TeV}$ for central PbPb collisions, $\sigma^{\mathrm{soft}} = 32\,\mathrm{mb}$

Table 4.

σ^{soft} mb	$\sqrt{S}$ GeV	$\bar{N}_{\mathrm{PbPb}}$	$\sqrt{\langle \delta E^2 \rangle}$ GeV	$\sqrt{p_1/\bar{N}}$	a		
					$\delta\phi = \pi$	$\delta\phi = \pi/2$	$\delta\phi = \pi/4$
0	200	75.7	21	0.084	0.088	0.124	0.178
	5500	87.4	84	0.086	0.094	0.133	0.189
32	200	17.1	14	0.168	0.177	0.259	0.387
	5500	47.1	74	0.117	0.127	0.180	0.257

Note that all the data presented in Table 4 include contributions from the singular points $r = -1, 0, 1$.

Let us now turn to the analysis of the results presented in Figs. 7–11 and Tables 3 and 4. The main goal is to understand the dependence of the angular pattern of the transverse energy flow on the basic parameters such as the infrared cutoff E_0, the total number of minijet-generating collisions $\bar{N}$, the yield of asymmetric pp collisions p_1 and the CMS energy $s^{1/2}$.

In the fourth column in Table 4 we show the quadratic mean $\langle \delta E^2 \rangle$ for the azimuthal opening $\delta\phi = \pi$. The results agree with (21), so that the average lack of balance in the transverse energy is indeed essentially determined by E_0 and $\bar{N}$.

To understand the results for the normalized asymmetry $p(r)$ it is helpful to consider a simplified model, in which the elementary pp collisions can produce only some given amount of transverse energy,

$$\left(\frac{\mathrm{d}\sigma}{\mathrm{d}E_\perp}\right)^{pp} = \sigma^{\mathrm{hard}}(\sqrt{s})\,\delta(E_\perp - E_0(\sqrt{s})), \qquad (25)$$

so that all transverse energy is assumed to be produced exactly at the cutoff E_0. Note that except for ascribing the energy production to elementary pp collisions, this model is very similar to the expected pattern of transverse energy production in the quasiclassical approach based on McLerran–Venugopalan model, cf. [21]. Then, for the considered azimuthal apertures $\delta\phi = \pi/2^n$ $(n = 0, 1, 2)$ we get for the standard deviation a defined in (24)[4]:

$$a\left(\delta\phi = \frac{\pi}{2^n}\right) \approx \sqrt{\frac{1}{2^n}\frac{p_1}{\bar{N}}}\left(1 + O\left(\frac{1}{\bar{N}}\right)\right). \qquad (26)$$

This shows that the width of the distribution $p(r)$ is determined by the ratio of the relative yield of asymmetric collisions p_1 to the average number of collisions. In Table 4 we compare the predictions of this simple model to the values of the standard deviation a computed using the differential spectra plotted in Figs. 2 and 2 (to save space, only the results for $\delta\phi = \pi$ are given in column 5) and observe only a 10% difference. This shows that the results obtained using the continuous spectra in Figs. 2 and 2 are essentially determined by the contribution at the cutoff energy E_0.

From Fig. 9 we see that for a small number of asymmetric collisions the shape of $p(r)$ has peculiar sharp peaks at certain values of r. The origin for this is in fact the growth of the differential cross section for transverse energy production at small $E_\perp$ in pp collisions, cf. Figures 2 and 2. Indeed, let us, for simplicity, assume that each pp collision in the restricted minijet ensemble can produce the transverse energy exactly at the cutoff $E_\perp = E_0$ only, cf. (25). In this case in addition to the "true" singular points $r = -1, 0, 1$ we will have "semisingular" ones so that for a particular event containing n minijets, with $n_{1\uparrow}$ being the number of "up-coming" one-jet events, $n_{1\downarrow}$ being the number of "down-coming" one-jet events, and $n_2 = n - n_{1\uparrow} - n_{1\downarrow}$ being the number of two-jet events, the following exact relation holds:

$$r = \frac{n_{1\uparrow} - n_{1\downarrow}}{n}. \qquad (27)$$

Thus the values of r belong to a set of *rational* numbers in the interval $[-1, 1]$, which we call "semisingular". Of course, the most spectacular "semisingular" points are those with small numerators and denominators both due to the higher frequency of events having a small number of minijets and to a smaller distribution width (deviation from $E_\perp = nE_0$) for events with a small number of asymmetric collisions.

Let us note that the appearance of the singular points $-1, 0, 1$ is a consequence of calculating the cross sections for the transverse energy production in the elementary hard block in the lowest order in perturbation theory. In the next-to-leading order, where the transverse energy can be shared between three (mini)jets, these singular points will become milder singularities of $p(r)$ at $r = -1, 0, 1$. This shows that the calculation of the true shape of $p(r)$ near the singular points requires, as usual, resumming the perturbative contributions to all orders.

Physically, within the scheme adopted in this paper, the number of semihard collisions depends on the sharing of inelasticity between soft and hard mechanisms of the transverse energy production. In the mixed scenario we assumed that 32 mb of the inelastic cross section of pp collisions corresponds to the soft production mechanism, while the rest of the inelastic cross section is due to semihard production. In the hard scenario it is assumed that the semihard transverse energy production saturates all available inelasticity. It is to be expected that the distributions characterizing azimuthal asymmetry of the transverse energy production $p(r)$ defined in (23) will be wider in the mixed scenario than in the hard one. From Table 4 we see that this is indeed the case. At RHIC energies the standard deviation for mixed scenario is bigger than that in a hard one in the ratio $a^{\mathrm{mixed}}_{\mathrm{RHIC}}/a^{\mathrm{hard}}_{\mathrm{RHIC}} \simeq 2.0$–$2.1$. At LHC energies the effect is less pronounced, here $a^{\mathrm{mixed}}_{\mathrm{LHC}}/a^{\mathrm{hard}}_{\mathrm{LHC}} \simeq 1.3$–$1.4$. We see that with growing CMS energy the angular pattern of the minijet-generated transverse energy flow is becoming less sensitive to the relative weight of perturbative and nonperturbative contributions to the inelastic cross section.

The dependence of the standard deviation a on the aperture remains essentially the same for both CMS energies and values of the impact parameter considered and is inversely proportional to the angular opening:

$$a_{\pi/2n} \simeq 2^{n/2} a_\pi, \qquad (28)$$

which is consistent with the prediction of the simple model of transverse energy production (26) and corresponds to a purely statistical change in the standard deviation, where shrinking the angular aperture by a factor of 2 enlarges the standard deviation by a factor of $2^{1/2}$.

4 Conclusions

The main results of our analysis can be formulated as follows.

We first discussed the basic asymmetry in the minijet transverse energy production in a restricted rapidity window in pp collisions due to different probabilities of having a "symmetric" two-jet or "asymmetric" one-jet contribution in the rapidity interval under consideration. The cross sections for symmetric and asymmetric contributions in pp collisions for RHIC and LHC energy show that while at RHIC energy the weight of both configurations is approximately equal, at LHC energy the asymmetric contribution is clearly dominant.

We further considered a geometrical model for nuclear collisions in which they are described as an incoherent

[4] The details of this calculation can be found in the Appendix.

superposition of nucleon–nucleon ones. We discussed two possible partitions of the inelastic cross section in terms of soft and semihard contributions and analyzed the angular pattern of minijet-generated energy flow for central and peripheral nuclear collisions at RHIC and LHC energies. Specifically we considered probability distributions for transverse energy–transverse energy correlations in the oppositely azimuthally oriented cones with varying aperture. We show that the resulting distributions are essentially sensitive to the number of semihard collisions, which is in turn dependent on the above-mentioned partition of the inelastic cross section into contributions of different types, and on the (related) choice of the infrared cutoff. We also show that the results are very close to the predictions of the simple model in which all the transverse energy is produced directly at the infrared cutoff.

The approach developed in this paper could be further generalized to the analysis of the minijet-generated background oriented flow [35] (for the definition of the oriented flow and comprehensive discussion see e.g. [36]). In particular, as the importance of the minijet contribution is expected to grow with energy, the presence of the background oriented flow of purely fluctuational origin could increasingly influence the corresponding hadronic observables.

Another crucial issue is the dynamical evolution of the primordial partonic inhomogeneities in the course of parton–hadron conversion. In a recent study [37] it was shown that the seed inhomogeneity in the initial condition of the elliptic flow type for the hadronic RQMD code survives the freeze-out and is visible in final azimuthal distributions. This question is surely most important and will be discussed in a forthcoming publication [33].

Acknowledgements. We are grateful to K. Kajantie, G. Zinovjev, J. Schukraft, K. Eskola, I.M. Dremin, I.V. Andreev, J.-P. Blaizot, J.-Y. Ollitrault, L. McLerran and P. Jacobs for useful discussions. A.L. is grateful for kind hospitality and support at CERN Theory Division, where this work was started, and at Service de Physique Theorique de Saclay, where the major part of it was done. We are grateful to the referee of the first version of this paper for constructive remarks and suggestions. This work was also partially supported by the Russian Fund for Basic Research, Grant 96-02-16347. The work of D.O. was partially supported by the INTAS grant 96-0457 within the ICFPM program.

Appendix

A $\langle r^2 \rangle$ calculation

In this Appendix we present a derivation of the formula for the standard deviation a, (26).

Let n be the number of minijet producing hadron–hadron collisions in a given nucleus–nucleus one characterized by the Poissonian distribution (9). Let us further denote by n_1 the number of those minijet producing hadron collisions in which only one minijet hits the rapidity window under consideration (asymmetric contribution), and by $n_{1\uparrow}$ and $n_{2\downarrow}$ the numbers of such single minijets propagating into the upper and lower of the two oppositely oriented cones, respectively. In what follows we shall use a simplified model of the transverse energy production, in which it is produced strictly at the cutoff E_0, cf. (25). The averaging over the event ensemle has to be done in the sequence opposite to the one adopted in the Monte Carlo procedure. First, we average over $n_{1\uparrow}$ at fixed $n_1 = n_{1\uparrow} + n_{1\downarrow}$:

$$\langle r^2 \rangle_{n_1} = \sum_{n_{1\uparrow}=0}^{n_1} \frac{1}{2^{n_1}} C_{n_1}^{n_{1\uparrow}} \frac{(n_{1\uparrow} - n_{1\downarrow})^2}{n^2} = \frac{n_1}{n^2}. \qquad (29)$$

Next, we average over n_1 at fixed n according to the binomial probability distribution (19):

$$\langle r^2 \rangle_n = \frac{p_1}{n}. \qquad (30)$$

Finally, we have to average over the Poissonian distribution (9) yielding

$$a^2 = \langle r^2 \rangle_n = \mathrm{e}^{-\bar{N}} \sum_{n=1}^{\infty} \frac{p_1}{n} \frac{\bar{N}^n}{n!} = p_1 \bar{N} \mathrm{e}^{-\bar{N}} F(1,1;2,2;\bar{N})$$
$$\approx \frac{p_1}{\bar{N}} \left(1 + O\left(\frac{1}{\bar{N}}\right)\right), \qquad (31)$$

where $F(1,1;2,2;\bar{N})$ is a generalized hypergeometric function.

References

1. S.A. Bass, M. Gyulassy, H. Stoecker, W. Greiner, J. Phys. G **25**, R1 (1999)
2. E.M. Levin, M.G. Ryskin, Phys. Rep. **189**, 267 (1990)
3. X.-N. Wang, Phys. Rep. **280**, 287 (1997)
4. K.J. Eskola, Comments. Nucl. Part. Phys. **22**, 185 (1998); K.J. Eskola, Minijets in ultrarelativistic heavy ion collisions at RHIC and LHC, hep-ph/9610365
5. K. Kajantie, P.V. Landshoff, J. Lindfors, Phys. Rev. Lett. **59**, 2527 (1987)
6. K.J. Eskola, K. Kajantie, J. Lindfors, Nucl. Phys. B **323**, 37 (1989)
7. K.J. Eskola, K. Kajantie, V. Ruuskanen, Eur. Phys. J. C **1**, 627 (1998)
8. K.J. Eskola, K. Kajantie, Zeit. Phys. C **75**, 515 (1997)
9. K.J. Eskola, K. Kajantie, P.V. Ruuskanen, K. Tuominen, Nucl. Phys. B **570**, 379 (2000)
10. T. Sjostrand, M. van der Zijl, Phys. Rev. D **36**, 2019 (1987)
11. J.P. Blaizot, A.H. Mueller, Nucl. Phys. B **289**, 847 (1987)
12. L. McLerran, R. Venugopalan, Phys. Rev. D **52**, 2233 (1994); ibid. D **49**, 2225 (1995)
13. A. Kovner, L. McLerran, H. Weigert, Phys. Rev. D **52**, 3809 (1995); ibid. D **52**, 6231 (1995)
14. Yu.V. Kovchegov, D.H. Rischke, Phys. Rev. C **56**, 1084 (1997)
15. S.G. Matinyan, B. Mueller, D.H. Rischke, Phys. Rev. C **56**, 1927 (1997); ibid. C **57**, 2197 (1998)
16. M. Gyulassy, L. McLerran, Phys. Rev. C **56**, 2219 (1997)

17. Yu. Kovchegov, A. Mueller, Nucl. Phys. B **329**, 451 (1998)
18. A. Krasnitz, R. Venugopalan, Real time simulations of high energy nuclear collisions, hep-ph/9808332; Nonperturbative computation of gluon minijet production in nuclear collisions at very high energies, hep-ph/9809433; Making glue in high energy nuclear collisions, hep-ph/9905319; The initial energy density of gluons produced in very high energy nuclear collisions, hep-ph/9909203
19. S.A. Bass, B. Mueller, W. Poeschl, J. Phys. G **25**, L109 (1999)
20. W. Poeschl, B. Mueller, Gluon field dynamics in ultra-relativistic heavy-ion collisions: evolution on a gauge lattice in 3+1 dimensions, nucl-th/9808031; Gauge lattice simulation of the soft QGP dynamics in ultra-relativistic heavy-ion collisions, hep-ph/9811441; Real-time evolution of soft gluon field dynamics in ultra-relativistic heavy-ion collisions, nucl-th/9903050
21. A.H. Mueller, Toward equilibration in the early stages after a high energy heavy ion collision, hep-ph/9906322; The Boltzmann equation for gluons at early times after a heavy ion collision, hep-ph/9909388
22. L. McLerran, Three lectures on the physics of small x and high gluon density, hep-ph/9903536
23. A.H. Mueller, Small-x physics, high parton densities and parton saturation in QCD, hep-ph/9911289
24. R. Stock, Analysis of single events in ultrarelativistic nuclear collisions, Proceedings Pre-Conference Workshop Quark Matter 95UCRL-TD-121571
25. E. Shuryak, C.M. Hung, Phys. Rev. C **57**, 397 (1997)
26. M. Gazdzicki, A. Leonidov, G. Roland, Eur. Phys. J. C **6**, 365 (1999)
27. M. Stephanov, K. Rajagopal, E. Shuryak, Event-by-event fluctuations in heavy ion collisions and the QCD critical point, hep-ph/9903292
28. A. Leonidov, D. Ostrovsky, Minijet transverse energy production in next-to-leading order in hadron and nuclear collisions, hep-ph/9811417
29. M. Gyulassy, D. Rischke, B. Zhang, Nucl. Phys. A **613**, 397 (1997)
30. X.-N. Wang, M. Guylassy, Phys. Rev. D **44**, 3501 (1991); ibid. D **45**, 844 (1992); Comp. Phys. Commun. **83**, 307 (1994)
31. A.D. Martin, R.G. Roberts, W.J. Stirling, Phys. Lett. B **354**, 155 (1995)
32. A. Bohr, B.R. Mottelson, Nuclear structure I (Benjamin, New York 1969) pp. 160, 223
33. A. Leonidov, D. Ostrovsky, in preparation
34. UA4 Collab., M. Bozzo et al., Phys. Lett. B **147**, 392 (1984); UA5 Collab., G.J. Alner et al., Z. Phys C **32**, 153 (1986); Fermilab E710 Collab., N. Amos et al., Phys. Rev. Lett. **63**, 2784 (1989); R.M. Baltrusaitis et al., Phys. Rev. Lett. **52**, 1380 (1984)
35. A. Leonidov, J.-Y. Ollitrault, D. Ostrovsky, in preparation
36. J.-Y. Ollitrault, Flow systematics from SIS to SPS energies, nucl-ex/9802005
37. F. Wang, H. Sorge, Remnants of initial anisotropic high energy density domains in nucleus–nucleus collisions, nucl-th/9811006